Title: Diberyllocene

Authors: Josef T. Boronski*[1], Agamemnon E. Crumpton[1], Lewis L. Wales[1], Simon Aldridge*[1]

Affiliations: 1) Chemistry Research Laboratory, Department of Chemistry, Oxford, OX1 3TA, U.K

*Corresponding author. Email: josef.boronski@sjc.ox.ac.uk; simon.aldridge@chem.ox.ac.uk

One-Sentence Summary: A stable compound featuring a beryllium-beryllium bond is reported, its geometric structure determined and its reactivity in the formation of M-Be bonds explored.

Abstract: The complex diberyllocene, CpBeBeCp (Cp = cyclopentadienyl anion), has been the subject of numerous quantum chemical investigations over the past five decades, yet has eluded experimental characterization. Here we report preparation and isolation of the compound by the reduction of beryllocene ($BeCp_2$) with a dimeric magnesium(I) complex and determination of its structure in the solid state by X-ray crystallography. Diberyllocene acts as a two-electron reductant in reactions that form beryllium-aluminum and -zinc bonds. Quantum chemical calculations indicate parallels between the electronic structure of diberyllocene and the simple homodiatomic species diberyllium (Be_2).

Main Text: Due to the extreme biotoxicity of beryllium, its chemistry is the least well-developed of all the non-radioactive elements.(*1–3*) This toxicity is a manifestation of beryllium's unique chemical properties – it forms the smallest of all metal ions (Be^{2+}; ionic radius, 0.31 Å; cf. Li^+ 0.60 Å), with unparalleled charge density (6.45 $Å^{-1}$; cf. Li^+, 1.67 $Å^{-1}$). Its bonding interactions often feature significant covalent character on account of the highly polarizing properties of the dication.(*2*) Given this capacity for covalency, the fundamental nature of beryllium-beryllium bonding has been debated for more than a century.(*4–11*) Basic molecular orbital theory predicts that diberyllium (Be_2) should have a bond order of zero, and only recently has meaningful insight into the true nature of the beryllium-beryllium interaction in gaseous Be_2 been obtained.(*12*,*13*) Moreover, despite seminal reports of zinc-zinc and magnesium-magnesium bonds in the early 2000s, and a host of quantum chemical investigations into the potential stability of beryllium-containing analogues, the isolation of a compound featuring a beryllium-beryllium bond in the condensed phases has not been achieved.(*14–17*)

Given the dearth of compounds featuring beryllium-beryllium bonds, in recent years, synthetic studies have focused on the preparation of low-valent beryllium species stabilized by redox non-innocent carbene ligands.(*18–20*) Compounds proposed to contain beryllium in the 0 and +1 oxidation states have been synthesized. However, such descriptions have proved controversial and are a source of ongoing debate within the literature.(*21–24*) We recently reported the beryllium-aluminyl complex CpBeAl(NON) (**1**, NON = 4,5-bis(2,6-diisopropylanilido)-2,7-di-tert-butyl-9,9-dimethylxanthene; Cp = cyclopentadienyl anion, $[C_5H_5]^-$), which displays reactivity expected from low-valent, nucleophilic beryllium.(*25–27*) Here we present diberyllocene, CpBeBeCp (**2**), an unambiguous beryllium(I) compound which is stable in the condensed phases and features a Be-Be bond. The experimentally determined properties of diberyllocene (which is stable at 80 ^oC for extended periods)

validate past quantum chemical predictions of its stability with respect to disproportionation to Be(0) and $BeCp_2$.(*7*)

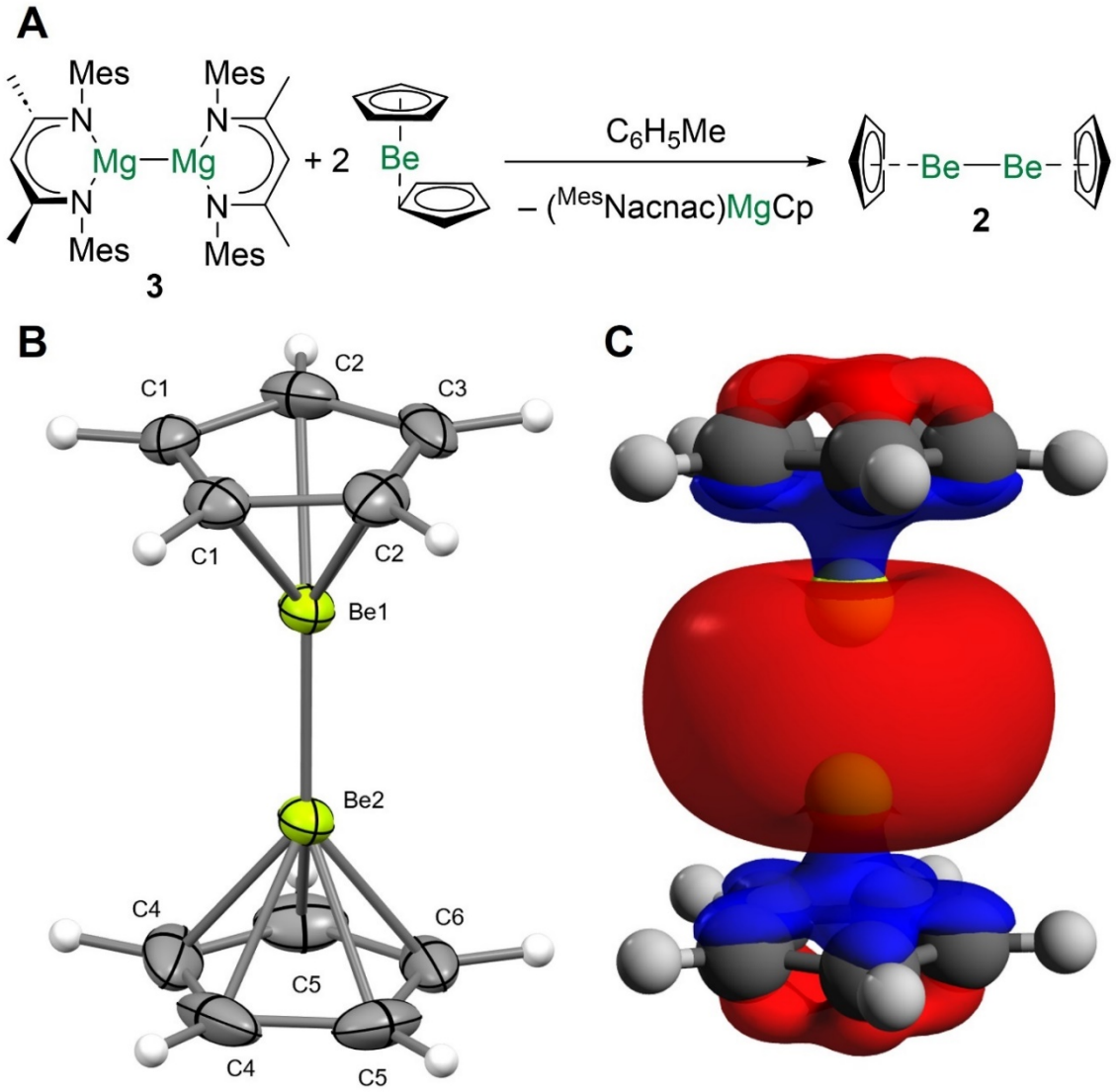

Figure 1: Synthesis, crystallographic, and electronic structure of diberyllocene (**2**). A) Synthesis of **2** via reaction of magnesium(I) complex **3** and beryllocene; B) Molecular structure of **2** in the solid state, as determined by x-ray crystallography. Thermal ellipsoids set at 50% probability; C) Calculated highest occupied molecular orbital for **2** (isovalue: 0.03 a.u.).

Synthesis and characterization. We previously succeeded in employing beryllocene $BeCp_2$ for the synthesis of beryllium-aluminyl complex **1**.(*25*, *28*) Calculations indicate compound **1** features a higher partial positive charge at aluminium than beryllium. Thus, the formation of **1** could be viewed as a reduction of beryllium(II) to beryllium(I) by the aluminyl anion, with associated one-electron oxidation of aluminum(I), forming a covalent Be-Al bond. We therefore set out to examine the possibility of reducing beryllocene to form a covalent Be-Be bond between two beryllium(I) centres. We turned our attention to di-magnesium(I) reagent $[(^{Mes}Nacnac)Mg]_2$ (**3**, $^{Mes}Nacnac$ = $[(MesNCMe)_2CH]^-$, Mes = 2,4,6-trimethylphenyl) which has been used for the controlled reduction of various organometallic compounds.(*6*,*17*) At room temperature, under an inert atmosphere, reaction of one equivalent of **3** with two

equivalents of $BeCp_2$ in toluene leads to quantitative formation of diberyllocene CpBeBeCp (**2**) and (^{Mes}Nacnac)MgCp, as indicated by multinuclear NMR spectroscopy (Figure 1 and S5). Both compounds are highly soluble in alkane solvents, such as pentane and hexane. However, **2** is a volatile solid and can be purified by sublimation at room temperature, allowing for its isolation in 85% yield.

Compound **2** can be crystallized from a concentrated hexane solution, yielding crystals suitable for the elucidation of its structure via single crystal X-ray diffraction (Figure 1B). Compound **2** is shown to feature two half-sandwich (cyclopentadienyl)beryllium units linked via a beryllium-beryllium bond. Zinc is the only other element for which the dimetallocene structural motif has been reported – for example in Cp*ZnZnCp* (**4**, Cp* = pentamethylcyclopentadienyl anion $[C_5Me_5]^-$) – and the configuration of **2** closely resembles that of **4**.(*14*,*15*) Both **2** and **4** display D_{5h} symmetry in the solid state, with the cyclopentadienyl ligands adopting a parallel, eclipsed configuration. At 2.0545(18) Å, the Be1-Be2 distance in **2** is in line with the sum of the single bond covalent radii for beryllium (2.04 Å).(*29*) This value is extremely close to that predicted by previous computational investigations of this compound (2.041 – 2.077 Å).(*7*–*9*) Examples of hydride-bridged beryllium compounds of the form $XBe(\mu\text{-}H)_2BeX$ all feature wider Be-Be separations (range: 2.098(3) – 2.212(8) Å; mean: 2.136 Å).(*26*,*30*–*32*) The Be-C distances within **2** range from 1.923(2) – 1.938(2) Å (mean: 1.930 Å), and are significantly longer than that of $BeCp_2$ (range: 1.862(9) – 1.936(8) Å; mean: 1.904 Å).(*28*) Consistently, the Be-(η^5-C_5H_5) centroid distances for Be1 and Be2 are both 1.519 Å, which is again significantly longer than that reported for $BeCp_2$ (1.485 Å). These bond metrics reflect the lower oxidation state and greater ionic radius of the beryllium(I) centres in **2**, compared with the beryllium(II) centre in $BeCp_2$.

Compound **2** was investigated by multinuclear nuclear magnetic resonance (NMR) spectroscopy. The ^{1}H NMR spectrum of **2** consists of a single resonance at 5.73 ppm, corresponding to the five equivalent cyclopentadienyl ligand protons. The ^{1}H NMR resonances of terminal beryllium-bound hydride ligands are generally found between 4 and 5 ppm.(*32*,*33*) Thus, **2** shows no signals attributable to Be-H hydrides in its ^{1}H NMR spectrum, only the resonance corresponding to the cyclopentadienyl ligand. Similarly, the ^{13}C NMR spectrum of **2** features one signal at 102.7 ppm. Compound **2** was also investigated by ^{9}Be NMR spectroscopy – which offers a convenient probe the electron density at the beryllium center – and shows a single high-field resonance at –27.6 ppm.(*25*,*34*) The coordination of strongly electron donating anionic ligands to beryllium generally shifts the ^{9}Be NMR resonances further upfield, as the increasingly electron-rich beryllium center becomes more strongly shielded. So, for example, whilst CpBeCl exhibits a $\delta_{^9Be}$ shift of –19.5 ppm, the corresponding signals of CpBeMe, CpBeGa(NON), CpBe[$Si(CH_3)_3$], and beryllium-aluminyl compound **1** are found at –20.5 ppm, –26.9 ppm, –27.7 ppm, and –28.8 ppm, respectively (Table S2).(*34*) These data suggest that the beryllium centre in **2** is similarly electron rich to that in **1**, consistent with the description of **2** as a metal-metal bonded beryllium(I) compound.(*25*, *34*) Moreover, the ^{9}Be NMR shift for compound **2** also provides evidence against a bridging hydride formulation for this compound, as such a species would be expected to show a much lower field chemical shift (Figure S23).(*34*)

To further argue against the hydride formulation for **2**, attenuated total reflection infrared (ATR IR) spectra were measured for samples of **2** prepared in both protio and perdeutero toluene solvents (Figure S14 and S15). The spectra are identical and neither features an absorbance band in the 1500 to 2000 cm^{-1} region where a Be-H stretch might be expected to

be observed.(*35*) The infrared spectra of both **2** and the hypothetical complex CpBe(μ-H)$_2$BeCp were simulated via quantum chemical calculations (Figure S17 and S18). The experimentally derived ATR IR spectrum of **2** closely matches the spectrum calculated for this complex (Figure S19) and differs significantly from that of the hydride bridged species (Figure S20), which features a very intense band at 1527 cm^{-1} (υ_s(Be-H$_b$)). The beryllium(II) hydride compound (CpBeH)$_n$ is thermally fragile and has been reported to undergo ligand redistribution, forming BeCp$_2$ and BeH$_2$, within minutes at –10 ^{o}C.(*35*,*36*) This reactivity contrasts with the relative stability of **2**, which shows no obvious signs of degradation upon heating in solution at 80 ^{o}C for 48 hours.

Quantum Chemical Investigations. Quantum chemical calculations were performed on **2** (B3LYP D3BJ def2-TZVP def2/J), in light of the new experimental data which had been unavailable for previous theoretical investigations of this molecule.(*7–9*) Key structural parameters align well with those determined crystallographically (e.g. *d*(Be-Be) = 2.046 Å, c.f. 2.0545(18) Å). These calculations indicate that the energetic separation between the highest occupied molecular orbital (HOMO) and lowest unoccupied molecular orbital (LUMO) is 5.541 eV. The HOMO of **2** is calculated to be the Be-Be σ-bonding orbital, with some Be-Cp σ-bonding character (Figure 1C); the lower-lying HOMO-1 to HOMO-4 correspond to the Cp-Be π-bonding combinations. As with the homodiatomic molecule Be$_2$, the Be-Be σ* antibonding orbital (LUMO+1) of diberyllocene is calculated to be significantly lower in energy than the Be-Be π-bonding orbitals (LUMO+4 and LUMO+5) (Figures S27 and S29).(*12*,*13*) This implies that further reduction of **2** would lead to a weakening of the Be-Be interaction. Indeed, the Be-Be distance in Be$_2$ (2.45 Å) is significantly longer than that measured for **2** (2.0545(18) Å).(*12*, *13*) As such, the core of **2** could be considered to be a (cyclopentadienyl-stabilized) dication of diberyllium, [BeBe]$^{2+}$, which molecular orbital theory would predict to feature a beryllium-beryllium σ-bond and a formal bond order of one, as is found here.(*37*,*38*)

Natural bond orbital (NBO) calculations were employed to examine the bonding and charge distribution within **2**. Natural population analysis (NPA) indicates that the 2s valence orbital of each beryllium atom is significantly populated (0.98 electrons), with non-negligible population of the beryllium 2p orbitals (0.17 e). These data are consistent with a formal beryllium(I) oxidation state. NBO calculations suggest that the Be-Be bond comprises 93% 2s character and 7% 2p character, with each beryllium center contributing equally (50:50). A Wiberg bond index (WBI) of 0.90 is calculated for the Be-Be bonding interaction, i.e. slightly greater than the WBI calculated for the Al-Be bond of **1** (0.82).(*25*) The charge distribution in **2** was probed by both NPA and quantum theory of atoms in molecules (QTAIM) calculations. QTAIM analysis indicates a non-nuclear attractor is present for the Be-Be interaction, as has been indicated by previous theoretical studies of **2**, and yields a charge of +1.33 for each beryllium atom.(*8*) NPA charges at each beryllium center are significantly lower (+0.84), but these do not take into account the presence of the non-nuclear attractor. QTAIM calculations previously performed on **1** provide a charge of +1.39 for the beryllium centre in this compound, suggesting the beryllium centres in **1** and **2** are similarly electron rich. This is consistent with the similar ^{9}Be NMR shifts measured for the two compounds.(*25*, *34*)

Due to the high quality of the X-ray crystallographic data obtained for **2**, quantum-crystallographic methods were employed to gain further evidence that this compound does not feature bridging hydride ligands. It should be noted that, even without employing quantum crystallographic methods, there is insufficient residual electron density to account

for the presence of bridging hydride ligands (Figures S34 and S35). The NoSpherA2 method was employed; this technique allows for refinement of crystallographic data based on the partitioned wavefunction of a molecule, rather than the traditional approach of refining against a model in which electron density is considered as point charges associated with specific atoms (independent electron model, IEM).(*39*, *40*) Using NoSpherA2, essentially all electron density in the data collected for **2** is accounted for (Figure S31 and S32). Indeed, the electron density associated with the cyclopentadienyl C-H bonds can be clearly identified (Figure S35) and there is no residual electron density resulting from bridging hydride ligands (Figure S31 and S33).

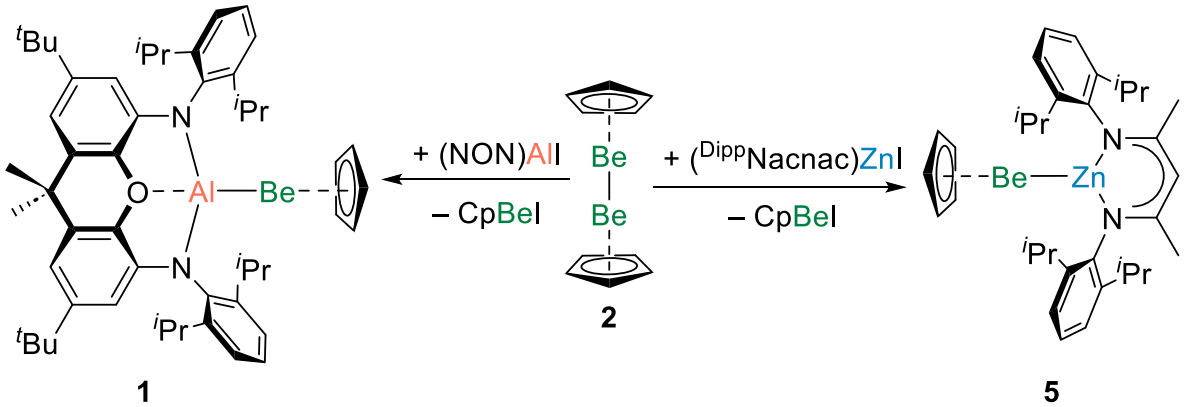

Figure 2: Reactivity of compound **2** with metal-iodide complexes, leading to the formation of beryllium-metal bonded complexes **1** and **5**.

Reactivity Studies. In view of the metal-metal bond in **2**, its reactivity as a source of low-valent beryllium was probed. Complex **2** does not react with H_2 (one atmosphere), even at elevated temperatures – a finding consistent with di-magnesium(I) compounds, such as **3**, which also do not react with H_2.(*17*) However, compound **2** reduces (NON)AlI, to cleanly and quantitatively yield the known beryllium-aluminyl compound **1** and CpBeI (Figure 2, left), evidencing the utility of **2** for the synthesis of beryllium-metal bonds.(*25*) This reactivity would not be expected from a beryllium(II) hydride compound. The reaction of **2** with (^{Dipp}Nacnac)ZnI (^{Dipp}Nacnac = $[(DippNCMe)_2CH]^-$, Dipp = 2,6-diisopropylphenyl) was similarly tested, to examine whether the formation of a (hitherto unknown) Zn-Be bond could be achieved (Figure 2, right). In a similar fashion, ^{1}H NMR spectroscopy indicates the complete consumption of **2**, along with quantitative formation of CpBeI and a new (^{Dipp}Nacnac)-containing species. Additionally, the formation of a small amount of dark grey metallic precipitate was observed. Crystallization from hexane yielded CpBeZn(^{Dipp}Nacnac) (**5**), which was structurally authenticated by single crystal X-ray diffraction (Figure S21).

The Zn-Be bond within compound **5** represents a very rare example of a beryllium-metal bonding combination, and provides further evidence for the constitution of **2** itself.(*25*,*27*,*41*) The Zn-Be bond distance within **5** (2.169(10) Å) is in line with the sum of the covalent radii of Be and Zn (2.20 Å), and is consistent with the presence of a covalent metal-metal bond.(*29*) Additionally, **5** exhibits a ^{9}Be NMR resonance (–27.65 ppm) consistent with a very electron rich beryllium metal centre, similar to **1** and **2**.(*25*,*34*) Quantum chemical calculations performed on **5** (B3LYP D3BJ def2-TZVP def2/J) yield a similar Zn-Be distance (2.175 Å) to that determined crystallographically and indicate that the HOMO is a Zn-Be sigma-bonding orbital (Figure S30). On the basis of the Pauling electronegativities of beryllium (1.57) and zinc (1.65), compound **5** might be assigned a beryllium(II)/zinc(0) formalism. However, quantum chemical calculations indicate significant covalent

contributions to the Zn-Be bonding in this compound, in similar fashion to the Be-Al bonding in **1**.(*25*) For example, NPA calculations imply that the valence orbitals of both zinc and beryllium are significantly populated (Be: 2s, 1.00 e; 2p, 0.16. Zn: 4s, 1.04 e). Additionally, NBO analysis suggests that beryllium and zinc make almost equal contributions to the Zn-Be bond (Zn:Be, 49.9:50.1). Thus, a beryllium(I)/zinc(I) formulation seems a more appropriate descriptor for **5**.

After half a century, diberyllocene (**2**) has been synthesized. The Be-Be distance in **2** (2.0545(18) Å) is in line with all previous quantum chemical investigations of this compound. Moreover, **2** reacts as a two-electron reductant and can be used to synthesize beryllium-metal bonds.

References and Notes:

1. R. Puchta, A brighter beryllium. *Nat. Chem.* **3**, 416 (2011).
2. D. Naglav, M. R. Buchner, G. Bendt, F. Kraus, S. Schulz, Off the Beaten Track—A Hitchhiker's Guide to Beryllium Chemistry. *Angew. Chemie - Int. Ed.* **55**, 10562–10576 (2016).
3. M. R. Buchner, Beryllium coordination chemistry and its implications on the understanding of metal induced immune responses. *Chem. Commun.* **56**, 8895–8907 (2020).
4. C. Jones, Open questions in low oxidation state group 2 chemistry. *Commun. Chem.* **3**, 8–11 (2020).
5. L. A. Freeman, J. E. Walley, R. J. Gilliard, Synthesis and reactivity of low-oxidation-state alkaline earth metal complexes. *Nat. Synth.* **1**, 439–448 (2022).
6. S. J. Bonyhady, C. Jones, S. Nembenna, A. Stasch, A. J. Edwards, G. J. McIntyre, β-Diketiminate-Stabilized Magnesium(I) Dimers and Magnesium(II) Hydride Complexes: Synthesis, Characterization, Adduct Formation, and Reactivity Studies. *Chem. - A Eur. J.* **16**, 938–955 (2010).
7. A. Velazquez, I. Fernández, G. Frenking, G. Merino, Multimetallocenes. A theoretical study. *Organometallics*. **26**, 4731–4736 (2007).
8. X. Li, S. Huo, Y. Zeng, Z. Sun, S. Zheng, L. Meng, Metal–Metal and Metal–Ligand Bonds in (η 5 -C 5 H 5) 2 M 2 (M = Be, Mg, Ca, Ni, Cu, Zn). *Organometallics*. **32**, 1060–1066 (2013).
9. Y. Xie, H. F. Schaefer, E. D. Jemmis, Characteristics of novel sandwiched beryllium, magnesium, and calcium dimers: C5H5BeBeC5H5, C 5H5MgMgC5H5, and C5H 5CaCaC5H5. *Chem. Phys. Lett.* **402**, 414–421 (2005).
10. S. A. Couchman, N. Holzmann, G. Frenking, D. J. D. Wilson, J. L. Dutton, Beryllium chemistry the safe way: A theoretical evaluation of low oxidation state beryllium compounds. *Dalt. Trans.* **42**, 11375–11384 (2013).
11. H. Schmidbaur, *Be Organoberyllium Compounds* (Springer Berlin Heidelberg, Berlin, Heidelberg, 1987; https://link.springer.com/book/10.1007/978-3-662-06024-7), vol. 21.
12. J. M. Merritt, V. E. Bondybey, M. C. Heaven, Beryllium dimer-caught in the act of bonding. *Science (80-.).* **324**, 1548–1551 (2009).
13. K. Patkowski, V. Špirko, K. Szalewicz, On the Elusive Twelfth Vibrational State of Beryllium Dimer. *Science (80-.).* **326**, 1382–1384 (2009).
14. I. Resa, E. Carmona, E. Gutierrez-Puebla, A. Monge, Decamethyldizincocene, a stable compound of Zn(I) with a Zn-Zn bond. *Science (80-.).* **305**, 1136–1138 (2004).
15. A. Grirrane, I. Resa, A. Rodriguez, E. Carmona, E. Alvarez, E. Gutierrez-Puebla, A. Monge, A. Galindo, D. del Río, R. A. Andersen, Zinc−Zinc Bonded Zincocene

Structures. Synthesis and Characterization of Zn 2 (η 5 -C 5 Me 5) 2 and Zn 2 (η 5 -C 5 Me 4 Et) 2. *J. Am. Chem. Soc.* **129**, 693–703 (2007).
16. S. P. Green, C. Jones, A. Stasch, Stable magnesium(I) compounds with Mg-Mg bonds. *Science (80-.).* **318**, 1754–1757 (2007).
17. C. Jones, Dimeric magnesium(I) β-diketiminates: a new class of quasi-universal reducing agent. *Nat. Rev. Chem.* **1**, 0059 (2017).
18. M. Arrowsmith, H. Braunschweig, M. A. Celik, T. Dellermann, R. D. Dewhurst, W. C. Ewing, K. Hammond, T. Kramer, I. Krummenacher, J. Mies, K. Radacki, J. K. Schuster, Neutral zero-valent s-block complexes with strong multiple bonding. *Nat. Chem.* **8**, 890–894 (2016).
19. C. Czernetzki, M. Arrowsmith, F. Fantuzzi, A. Gärtner, T. Tröster, I. Krummenacher, F. Schorr, H. Braunschweig, A Neutral Beryllium(I) Radical. *Angew. Chemie - Int. Ed.* **60**, 20776–20780 (2021).
20. G. Wang, J. E. Walley, D. A. Dickie, S. Pan, G. Frenking, R. J. Gilliard, A Stable, Crystalline Beryllium Radical Cation. *J. Am. Chem. Soc.* **142**, 4560–4564 (2020).
21. D. Jędrzkiewicz, J. Mai, J. Langer, Z. Mathe, N. Patel, S. DeBeer, S. Harder, Access to a Labile Monomeric Magnesium Radical by Ball□Milling. *Angew. Chemie Int. Ed.* **61** (2022), doi:10.1002/anie.202200511.
22. M. Gimferrer, S. Danés, E. Vos, C. B. Yildiz, I. Corral, A. Jana, P. Salvador, D. M. Andrada, The oxidation state in low-valent beryllium and magnesium compounds. *Chem. Sci.* **13**, 6583–6591 (2022).
23. M. Gimferrer, S. Danés, E. Vos, C. B. Yildiz, I. Corral, A. Jana, P. Salvador, D. M. Andrada, Reply to the 'Comment on "The oxidation state in low-valent beryllium and magnesium compounds"' by S. Pan and G. Frenking, Chem. Sci. , 2022, 13 , DOI: 10.1039/D2SC04231B. *Chem. Sci.* **14**, 384–392 (2023).
24. S. Pan, G. Frenking, Comment on "The oxidation state in low-valent beryllium and magnesium compounds" by M. Gimferrer, S. Danés, E. Vos, C. B. Yildiz, I. Corral, A. Jana, P. Salvador and D. M. Andrada, Chem. Sci. 2022, 13, 6583. *Chem. Sci.* **14**, 379–383 (2023).
25. J. T. Boronski, L. R. Thomas-Hargreaves, M. A. Ellwanger, A. E. Crumpton, J. Hicks, D. F. Bekiş, S. Aldridge, M. R. Buchner, Inducing Nucleophilic Reactivity at Beryllium with an Aluminyl Ligand. *J. Am. Chem. Soc.* **145**, 4408–4413 (2023).
26. A. Paparo, A. J. R. Matthews, C. D. Smith, A. J. Edwards, K. Yuvaraj, C. Jones, N-Heterocyclic carbene, carbodiphosphorane and diphosphine adducts of beryllium dihalides: synthesis, characterisation and reduction studies. *Dalt. Trans.* **50**, 7604–7609 (2021).
27. A. Paparo, C. D. Smith, C. Jones, Diagonally Related s- and p-Block Metals Join Forces: Synthesis and Characterization of Complexes with Covalent Beryllium–Aluminum Bonds. *Angew. Chemie - Int. Ed.* **58**, 11459–11463 (2019).
28. R. Fernández, E. Carmona, Recent developments in the chemistry of beryllocenes. *Eur. J. Inorg. Chem.*, 3197–3206 (2005).
29. P. Pyykkö, Additive covalent radii for single-, double-, and triple-bonded molecules and tetrahedrally bonded crystals: A summary. *J. Phys. Chem. A*. **119**, 2326–2337 (2015).
30. M. Arrowsmith, M. S. Hill, G. Kociok-Köhn, Activation of N-heterocyclic carbenes by {BeH2} and {Be(H)(Me)} fragments. *Organometallics*. **34**, 653–662 (2015).
31. G. W. Adamson, H. M. M. Shearer, The crystal structure of the etherate of sodium hydridodiethylberyllate. *Chem. Commun.*, 240 (1965).
32. T. J. Hadlington, T. Szilvási, Accessing the main-group metal formyl scaffold through CO-activation in beryllium hydride complexes. *Nat. Commun.* **13**, 2–11 (2022).

33. R. Han, G. Parkin, [Tris(3-tert-butylpyrazolyl)hydroborato]beryllium hydride: synthesis, structure, and reactivity of a terminal beryllium hydride complex. *Inorg. Chem.* **31**, 983–988 (1992).
34. P. G. Plieger, K. D. John, T. S. Keizer, T. M. McCleskey, A. K. Burrell, R. L. Martin, Predicting 9Be nuclear magnetic resonance chemical shielding tensors utilizing density functional theory. *J. Am. Chem. Soc.* **126**, 14651–14658 (2004).
35. M. del Mar Conejo, R. Fernández, E. Carmona, R. A. Andersen, E. Gutiérrez-Puebla, M. A. Monge, Synthetic, Reactivity, and Structural Studies on Half-Sandwich (η5-C5Me5)Be and Related Compounds: Halide, Alkyl, and Iminoacyl Derivatives. *Chem. - A Eur. J.* **9**, 4462–4471 (2003).
36. T. C. Bartke, A. Bjorseth, A. Haaland, K.-M. Marstokk, H. Møllendal, Microwave spectrum, structure and dipole moment of cyclopentadienylberyllium hydride. *J. Organomet. Chem.* **85**, 271–277 (1975).
37. C. A. Nicolaides, P. Valtazanos, Hydrogen complexes of Be2+2. *Chem. Phys. Lett.* **174**, 489–493 (1990).
38. A. Kalemos, The nature of the chemical bond in Be2+, Be2, Be2-, and Be3. *J. Chem. Phys.* **145** (2016), doi:10.1063/1.4967819.
39. L. Midgley, L. J. Bourhis, O. V. Dolomanov, S. Grabowsky, F. Kleemiss, H. Puschmann, N. Peyerimhoff, Vanishing of the atomic form factor derivatives in non-spherical structural refinement – a key approximation scrutinized in the case of Hirshfeld atom refinement. *Acta Crystallogr. Sect. A Found. Adv.* **77**, 519–533 (2021).
40. F. Kleemiss, O. V. Dolomanov, M. Bodensteiner, N. Peyerimhoff, L. Midgley, L. J. Bourhis, A. Genoni, L. A. Malaspina, D. Jayatilaka, J. L. Spencer, F. White, B. Grundkötter-Stock, S. Steinhauer, D. Lentz, H. Puschmann, S. Grabowsky, Accurate crystal structures and chemical properties from NoSpherA2. *Chem. Sci.* **12**, 1675–1692 (2021).
41. H. Braunschweig, K. Gruss, K. Radacki, Complexes with dative bonds between d- and s-block metals: Synthesis and structure of [(Cy3P)2Pt-Be(Cl)X] (X = Cl, Me). *Angew. Chemie - Int. Ed.* **48**, 4239–4241 (2009).
42. J. T. Boronski, Diberyllocene: xyz-coordinates of optimized structures. *Dryad, Dataset* (2023), doi:10.5061/dryad.kwh70rz8n.
43. M. R. Buchner, M. Müller, Handling Beryllium, the Safe Way. *ACS Chem. Heal. Saf.* **30**, 36–43 (2023).
44. J. Hicks, P. Vasko, J. M. Goicoechea, S. Aldridge, Synthesis, structure and reaction chemistry of a nucleophilic aluminyl anion. *Nature*. **557**, 92–95 (2018).
45. M. P. Blake, N. Kaltsoyannis, P. Mountford, Synthesis, molecular and electronic structure, and reactions of a Zn-Hg-Zn bonded complex. *Chem. Commun.* **51**, 5743–5746 (2015).
46. J. Cosier, A. M. Glazer, A nitrogen-gas-stream cryostat for general X-ray diffraction studies. *J. Appl. Crystallogr.* **19**, 105–107 (1986).
47. Agilent Technologies, CrysAlisPro.
48. G. M. Sheldrick, SHELXT – Integrated space-group and crystal-structure determination. *Acta Crystallogr. Sect. A Found. Adv.* **71**, 3–8 (2015).
49. G. M. Sheldrick, Crystal structure refinement with SHELXL. *Acta Crystallogr. Sect. C Struct. Chem.* **71**, 3–8 (2015).
50. O. V. Dolomanov, L. J. Bourhis, R. J. Gildea, J. A. K. Howard, H. Puschmann, OLEX2 : a complete structure solution, refinement and analysis program. *J. Appl. Crystallogr.* **42**, 339–341 (2009).
51. F. Neese, The ORCA program system. *WIREs Comput. Mol. Sci.* **2**, 73–78 (2012).
52. F. Neese, F. Wennmohs, U. Becker, C. Riplinger, The ORCA quantum chemistry

program package. *J. Chem. Phys.* **152**, 224108 (2020).
53. S. Grimme, S. Ehrlich, L. Goerigk, Effect of the damping function in dispersion corrected density functional theory. *J. Comput. Chem.* **32**, 1456–1465 (2011).
54. E. Caldeweyher, S. Ehlert, A. Hansen, H. Neugebauer, S. Spicher, C. Bannwarth, S. Grimme, A generally applicable atomic-charge dependent London dispersion correction. *J. Chem. Phys.* **150**, 154122 (2019).
55. E. D. Glendening, J. K. Badenhoop, A. E. Reed, J. E. Carpenter, B. J. A., C. M. Morales, P. Karafiloglou, C. R. Landis, F. Weinhold, NBO 7.0 (2018).
56. T. Lu, F. Chen, Multiwfn: A multifunctional wavefunction analyzer. *J. Comput. Chem.* **33**, 580–592 (2012).

Acknowledgments:

Funding: J.T.B. is thankful to St John's College, Oxford, for a Junior Research Fellowship. We thank the John Fell Fund (0011792) for financial support. We thank the EPSRC Centre for Doctoral Training in Inorganic Chemistry for Future Manufacturing (OxICFM, EP/S023828/1 studentship for L.L.W. and A.E.C.). Author contributions: J.T.B.: conceptualization, investigation, visualisation, writing – original draft, writing – review & editing, funding acquisition, supervision, and project administration. A.E.C.: quantum crystallographic investigations, writing – review & editing. L.L.W.: collection and processing of X-ray crystallographic data, writing – review & editing. S.A.: visualisation, supervision, project administration, and writing – review & editing. Competing interests: The authors declare no competing interests. Data and materials availability: X-ray data are available free of charge from the Cambridge Crystallographic Data Centre under reference numbers CCDC 2245595 (**2**), 2245596 (**5**), and 2246346 ((^{Mes}Nacnac)MgCp). All other experimental, spectroscopic, crystallographic, and computational data are included in the supplementary materials. Computational data are also available via Dryad.(*42*)

List of Supplementary Materials:

Materials and Methods:
Fig. S1 to S35
Table S1 to S3
References (*43-56*)